Design of a Spherical Tensegrity Robot for Dynamic Locomotion

Kyunam Kim[1], Deaho Moon[2], Jae Young Bin[1], and Alice M. Agogino[1], *Senior Member, IEEE*

***Abstract*— This work presents a novel spherical tensegrity robot, T12-R, which is designed and prototyped based on a twelve-rod tensegrity structure that resembles a rhombicuboctahedron. The geometry of T12-R allows for fast rolling and a detailed description of the robot design is provided. A simulation study of T12-R shows that the robot is capable of performing static locomotion. Control strategies for achieving dynamic locomotion in hardware are discussed.**

I. Introduction

Naturally compliant tensegrity structures have several unique properties that are advantageous for co-robotic or soft robotic platforms; they are lightweight, deployable, robust, and safe. By leveraging these distinctive features of tensegrity structures, tensegrity robots have been envisioned for a wide range of new applications such as planetary exploration missions [1], [2].

Although tensegrity structures have existed more than sixty years since they were first invented and explored by early pioneers such as Buckminster Fuller and Kenneth Snelson [3], [4], they were only recently introduced to the field of robotics. Despite a relatively short history of using tensegrity structures as mobile robotic platforms, a number of hardware tensegrity robots with mobility have been introduced in the literature [5], [6], [7], [8], [9], [10], [11], [12], [13].

Many tensegrity structures have asymmetric and irregular shapes, but researchers have had a special interest in the structures that are spherical and used them as mobile robotic platforms [14], [15]. Here, the term "spherical" does not mean that the tensegrity structures have smooth spherical outer shapes, but rather it means that their outer shapes are similar to a sphere. Among the family of spherical tensegrity structures, a six-rod tensegrity structure is the simplest three-dimensional one and several hardware robots based on this structure have been introduced in the literature [1], [14], [16], [17]. Most of the research on these robots studied their mobility and developed controllers for their rolling either from hardware experiments [18], [6], [19], [20], or in simulations [8], [21], [22].

While being successful at rolling, tensegrity robots based on a six-rod tensegrity structure can only move at a low speed because of their geometric constraint. Their outer shapes prevent them from moving in a straight line, and this causes momentum loss, limiting their moving speed. To overcome this problem, a novel spherical tensegrity robot, T12-R (Fig. 1), that enables high speed rolling is presented in this work.

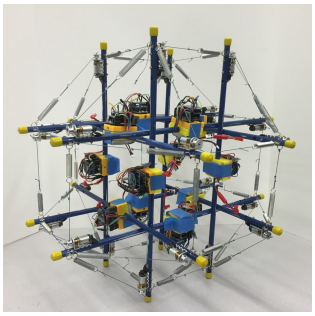

Fig. 1. T12-R, a rapidly prototyped tensegrity robot based on a twelve-rod tensegrity structure at the Berkeley Emergent Space Tensegrities laboratory, UC Berkeley†.

The rest of the paper is organized as follows. Section II presents motivations of the design of T12-R and Sect. III provides a detailed description of the design. A simulation study of T12-R for static locomotion is provided in Sect. IV, and control strategies for achieving dynamic locomotion of T12-R are discussed in Sect. V. The paper concludes with Sect. VI.

II. Motivation

Spherical tensegrity robots can move on the ground by rolling, which is realized by adjusting their centers of mass through deformation. The outer shape of a six-rod tensegrity robot resembles an icosahedron that consists of 20 triangles, and the outer shape of a twelve-rod tensegrity robot that will be presented in Sect. III is similar to a rhombicuboctahedron that consists of eight triangles and 18 squares (Fig. 2). Because the outer shapes of the robots are not smooth, their rolling motion is discontinuous and hence called *punctuated rolling*. A rotation from one face to the next face is referred to as a *step*. A more detailed description of rolling motion of spherical tensegrity robots is presented in [9].

Figure 3 shows the paths taken by an icosahedron-like six-rod tensegrity robot and a rhombicuboctahedron-like twelve-rod tensegrity robot when they are moving forward. Because the outer surface of a six-rod tensegrity robot consists of triangles only, the robot cannot roll in a straight line, rather it moves in a zig-zag way. While this behavior is acceptable for

*This work was supported by NASA's Early Stage Innovation grant NNX15AD74G.

[1]Kyunam Kim, Jae Young Bin, and Alice M. Agogino are with the Department of Mechanical Engineering, University of California at Berkeley, Berkeley, CA 94720 USA {knkim, jaeyoungbin, agogino}@berkeley.edu

[2]Deaho Moon is with the Department of Mechanical and Aerospace Engineering, University of California at Los Angeles, Los Angeles, CA 90095 USA dmoon0322@ucla.edu

†http://best.berkeley.edu/best-research/best-berkeley-emergent-space-tensegrities-robotics/

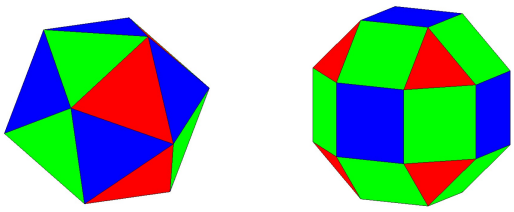

(a) Icosahedron (b) Rhombicuboctahedron

Fig. 2. A six-rod tensegrity robot has an outer shape similar to an icosahedron. T12-R, a twelve-rod tensegrity robot, has an outer shape similar to a rhombicuboctahedron.

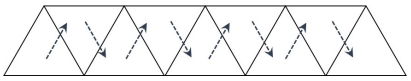

(a) Path of a six-rod tensegrity

(b) Path of a twelve-rod tensegrity

Fig. 3. The actual paths taken by six-rod and twelve-rod tensegrity robots when moving in a straight line. A six-rod tensegrity robot moves in a zig-zag way and switches its heading direction after each and every step. This causes large momentum loss and the structure is not suitable for fast rolling. On the other hand, a rhombicuboctahedron-like twelve-rod tensegrity robot has rectangles on its outer surface, which enables straight rolling and prevents loss of momentum.

rolling at slow speed, it is not desirable for high speed rolling because this robot will change its moving direction after each and every step, which will result in a large momentum loss. The zig-zag path can be avoided and rolling in a straight line can be achieved if the outer surface of a tensegrity robot mainly consists of rectangles in series. Indeed, a rhombicuboctahedron-like twelve-rod tensegrity structure is the simplest spherical tensegrity that has this property. For this reason, the robot presented in this paper is based on a rhombicuboctahedron-like twelve-rod tensegrity structure. The geometry of this robot prevents a momentum loss arising from repeated change of moving direction and enables high speed rolling.

There is another important advantage of having the outer surface similar to a rhombicuboctahedron. Because this geometry is symmetric about three mutually-orthogonal planes, if control is applied such that the robot's deformation maintains symmetry about one of these planes, then the motion of the robot can be described on the plane by projecting the structural members (i.e., rods and cables) onto the plane (Fig. 4). By exploiting this, the dimensions of state space and control inputs can be reduced, which will facilitate controller design and implementation.

Specifically, a slender rod, neglecting rotation about its axis of symmetry, has five degrees of freedom (DOF) in a three-dimensional space. Therefore, a six-rod tensegrity robot has 30-DOF and a twelve-rod tensegrity robot has 60-DOF. Here, it is assumed that the rods of the robots are not in contact, and they do not constrain motion of the other rods. Now, if we assume the symmetric deformation of the twelve-rod tensegrity robot and project the motion of the

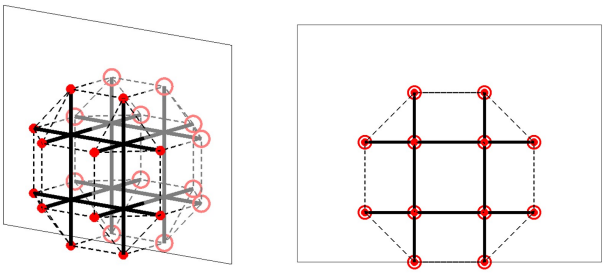

(a) A twelve-rod tensegrity (perspective view) (b) A twelve-rod tensegrity (projected view)

Fig. 4. A twelve-rod tensegrity structure that T12-R is based on has its outer geometry similar to a rhombicuboctahedron. This geometry is symmetric about three mutually-orthogonal planes one of which is shown in this figure. If the deformation of the structure is symmetric about this plane, then the shape and motion of the structure can be described on the plane by projecting the members of the structure onto the plane.

structural members onto the plane, then eight rods that are parallel to the symmetry plane have only three-DOF per rod, and the other four rods that are perpendicular to the plane have only two-DOF per rod on the plane. Furthermore, because the two rods that are mirrored about the plane always have the same motion, the total degrees of freedom for the eight parallel rods are halved from 24-DOF to 12-DOF. As a result, the twelve-rod tensegrity robot exploiting the symmetry has a total of 20-DOF. This is only one third of the original system's 60-DOF and is even smaller than the total degrees of freedom of a six-rod tensegrity structure that is the simplest spherical tensegrity structure. By exploiting this reduction in the total degrees of freedom, dynamics of the twelve-rod tensegrity robot can be compactly written, which will facilitate the robot's controller design.

Construction of dynamics models of different types of tensegrity structures has been extensively studied in the previous research [23], [24], [25], [26], [27], [28], [29]. The development of controllers for achieving dynamic rolling of the twelve-rod tensegrity robot, however, is ongoing research. A potential research direction in this regard is proposed in Sect. V.

III. Hardware Design of T12-R

To the best of authors' knowledge, all of the spherical tensegrity robots presented in the previous research are based on a six-rod tensegrity structure, and T12-R (Fig. 1) is the first spherical tensegrity robot that is based on a twelve-rod tensegrity structure. Yet, the hardware design of T12-R largely inherits the modular design of its predecessor, TT-3, a six-rod tensegrity robot developed at UC Berkeley [10].

T12-R is built with twelve aluminum tubes with lengths of 45 cm and outer diameters of 0.95 cm. Each rod includes a bundle of electronic components at the center, which includes controllers, batteries, and other electronics. Because the controllers are distributed across the rods, radio chips are also installed to enable wireless communication between the controllers (and a ground control station, if exists). By adopting the distributed control scheme, the center volume of the robot is cleared for an additional payload.

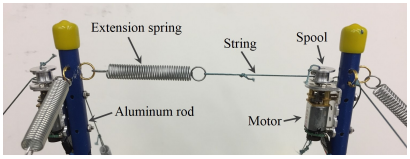

Fig. 5. An edge of T12-R consists of an extension spring and an unstretchable string that is spooled in and out by a motor.

TABLE I
PHYSICAL PARAMETERS OF T12-R

Total robot mass	1.78 kg
Rod length	45 cm
Rod mass (including motors and electronics)	132.9 g
Spring rest length	3.8 cm
Spring stiffness	771 N/m
Motor free-run speed at 6V	100 rpm
Motor stall torque at 6V	0.494 Nm

In order to provide actuation, 24 brushed DC motors are placed at the rod ends and are connected to the electronics located at the rod centers. The motors are connected to rigid strings through spools and change the lengths of edges by spooling the strings in and out (Fig. 5). The strings are connected to extension springs that provide compliance to the overall structure. As a result, the edges also change in tension when their lengths are changed due to motor actuation. The whole structure deforms when a set of motors are actuated to control the lengths of the associated edges.

Considering that T12-R has a total of 48 edges on its outer surface, 48 motors would be needed to make the robot fully-actuated, but only half of them are installed on the current prototype (one on each rod end). Yet, our simulation shows that it is possible to realize punctuated rolling with this underactuated system, as will be shown in Sect. IV. Each rod weighs 132.9 g including two motors and electronics. The total weight of T12-R is measured as 1.78 kg. Identical springs with a rest length of 3.8 cm and a stiffness of 771 N/m are used on all of the edges. The physical parameters of T12-R are summarized in Table I.

One downside of this design is that there exist points where three mutually-orthogonal rods meet. This is not desirable because the contact forces between the touching rods may affect the deformation characteristic of the overall structure and may put extra loads to the motors. To avoid this issue, the rods are placed apart from each other at such points so that they are no longer in contact when the robot deforms to realize a step. As a result of this setup, however, the outer shape of T12-R becomes slightly asymmetric.

IV. STATIC LOCOMOTION OF T12-R

In the authors' previous work, a systematic way of obtaining desirable deformations of a six-rod tensegrity robot was presented [30]. The obtained deformations, when implemented on a hardware robot, enabled stepping of the robot. The method does not limit itself to a six-rod tensegrity robot, and it can be applied to any spherical tensegrity robot satisfying one condition; rods of the robot do not touch each other. Tensegrity structures satisfying this condition is often categorized as *class 1* [31]. A six-rod tensegrity robot usually falls under this category as none of its rods are in contact unless the robot is extremely deformed. As mentioned at the end of Sect. III, the rods of T12-R are placed in a way that they do not touch each other when the robot deforms to realize a step. Therefore, T12-R can be considered as class 1 within its operation range.

The process of finding desirable deformations of class 1 spherical tensegrity robots presented in [30] relies on two methods: 1) dynamic relaxation, and 2) multi-generation Monte Carlo. Only a brief description of the methods is presented below. Equations and other technical details can be found in [30].

A. Dynamic Relaxation

Dynamic relaxation is a numerical method used for predicting deformations of tensegrity structures when their cable tensions are known. The method has been used for form-finding of wide-span cable nets and pre-stressed fabric membranes [32], [33]. Recently, the method was also applied to tensegrity structures to find their equilibrium shapes [34], [35]. The authors' previous work [30] builds on the previous research and use the dynamic relaxation to predict deformations of hardware tensegrity robots when their cable tensions are known. In that work, the method uses *kinetic damping* to dissipate kinetic energy from a system when the energy reaches a peak, shifting the system towards a lower energy state, eventually to a (local) equilibrium. The dynamic relaxation is used again in this work to predict deformations of T12-R when its cable tensions are given.

B. Multi-Generation Monte Carlo

In addition to the dynamic relaxation, a multi-generation Monte Carlo method is used to find good sets of cable tensions that will produce desirable deformations of T12-R for the realization of steps. In this method, a set of cable tensions are randomly created (within a physical bound) and the dynamic relaxation is run to find the resultant deformed shape of T12-R associated with this set of cable tensions. The obtained deformed shape then becomes a sample. In each generation, a number of samples are generated and evaluated, and the best sample is identified. The sampling in the following generation happens only in a neighborhood of the best sample from the previous generation, which helps to improve the sampling efficiency. In other words, only the deformed shapes that look similar to the best shape from the previous generation are sampled in the current generation.

A deformed shape is more unbalanced and is more likely to tip over, or perform a step, when its center of mass is located farther away from its supporting polygon. This idea is used to measure the quality of samples (Fig. 6); an evaluation function defined as a distance between the ground projection of the center of mass (GCoM) and the closest edge of the supporting polygon is used to assign a score to each sample. The score has the same magnitude of the distance, but it is

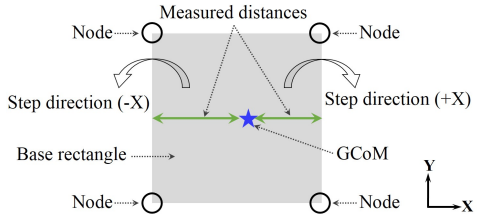

Fig. 6. The metric used for evaluation of deformed shapes of T12-R. Assuming that the robot intends to make a step in X-direction, distances between GCoM and two edges of a base rectangle are measured. The distance is positive if GCoM is within the base rectangle and negative otherwise. The deformed shape is assigned with a score equal to the smaller distance of the two.

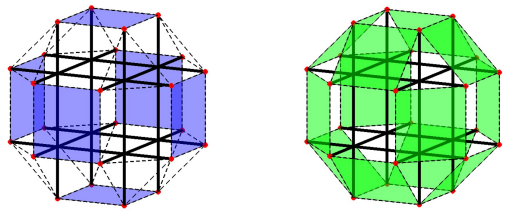

(a) Perpendicular rectangles (b) Diagonal rectangles

Fig. 7. The outer surface of T12-R consists of triangles and rectangles. There are six perpendicular and twelve diagonal rectangles.

given a positive (or negative) sign if GCoM stays inside (or outside) of the supporting polygon. Note that center of mass is used as an evaluation criterion. Because center of mass is a static property, the motion of T12-R realized by this approach can be considered as static locomotion.

C. Types of Steps

The outer surface of T12-R consists of eight triangles and two types of rectangles; 1) six *perpendicular rectangles* each of which is formed by four nodes of four parallel rods and is perpendicular to the rods, and 2) twelve *diagonal rectangles* each of which is formed by four nodes of two orthogonal pairs of parallel rods and is diagonal to the rods (Fig. 7). In this work, only the cases in which T12-R starts its step from a rectangular face and lands on another rectangular face are considered because triangular faces are not part of a straight path depicted in Fig. 3b. However, control strategies for realizing steps including triangular faces can be developed using the same method presented in this work. As a result, T12-R can perform two different types of steps.

- A *PD-step* leads the robot from a perpendicular base rectangle to an adjacent diagonal base rectangle.
- A *DP-step* leads the robot from a diagonal base rectangle to an adjacent perpendicular base rectangle.

D. Simulation

In order to find desirable deformations for each type of step, multi-generation Monte Carlo is run twice using the physical parameters of T12-R listed in Table I, and two actuation policies are developed separately in simulation. The simulation assumes that T12-R initially has a symmetric outer shape and all of its string lengths are set to 12 cm. This assumption is made to prevent bias in deformation

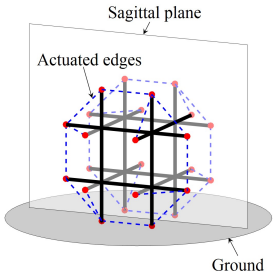

Fig. 8. The current prototype of T12-R has only 24 motors that are installed symmetric about the sagittal plane. The motors control the lengths of edges shown as blue dashed lines in this figure to change the shape of the structure.

that may occur due to asymmetric initial conditions. The assumption does not conflict with the fact that T12-R is designed to be slightly asymmetric in its neutral form to avoid contact between rods because the purpose of the simulation is to obtain final deformed shapes after applying actuation forces and the robot does not need to start from a symmetric shape to reproduce the deformed shapes. It is further assumed that the motors of T12-R can spool in (or out) the connected strings to the minimum (or maximum) length of $d_{min} = 8$ cm (or $d_{max} = 16$ cm). These values are chosen because the motors of T12-R are expected to operate safely within this range without significantly loading themselves. In the first generation of the Monte Carlo, string lengths are randomly sampled from a uniform distribution of $[d_{min},\ d_{max}]$, whereas for all of the later generations, string lengths are randomly sampled from a uniform distribution of $[\max(d_{min}, d^* - \delta d),\ \ \min(d_{max}, d^* + \delta d)]$, where d^* represents the string lengths of the best sample from the previous generation and $\delta d = 1$ cm. As a result, only the deformed shapes that look similar to the best shape of the previous generation are sampled.

It is further assumed that the total of 24 motors of T12-R are mounted symmetrically about its sagittal plane and each pair of motors that are mirrored about the plane are identically actuated (Fig. 8). As a consequence of this assumption, the input to the dynamic relaxation is a 12-dimensional vector of edge string lengths, where each length specifies the target lengths of two actuated edges that are mirrored to each other. For the multi-generation Monte Carlo, 100 samples are obtained per generation and a total of 10 generations are run to find the best deformed shape of T12-R for each of PD- and DP-steps.

Figure 9 shows the best deformed shapes of T12-R for realizing PD- and DP-steps obtained by the above method. Note that GCoMs of both shapes are outside of the supporting polygon, and thus the shapes are expected to enable PD- and DP-steps of T12-R. The implementation of this result on the hardware robot is currently work in progress.

V. Dynamic Locomotion of T12-R

The Monte Carlo based method presented in Sect. IV relies on GCoM, and therefore the motion realized by this method can be thought as static locomotion. T12-R has several advantages for dynamic locomotion as discussed in

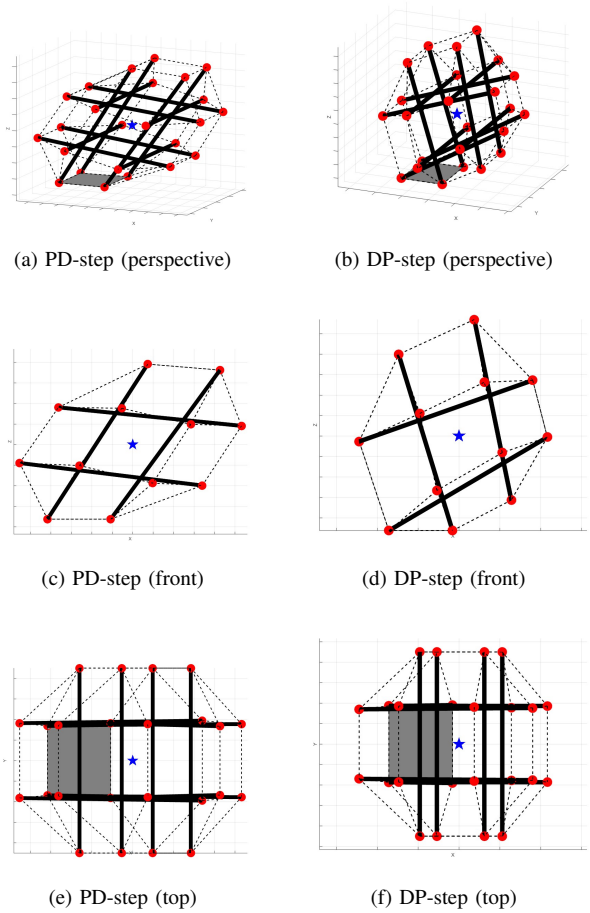

(a) PD-step (perspective) (b) DP-step (perspective)

(c) PD-step (front) (d) DP-step (front)

(e) PD-step (top) (f) DP-step (top)

Fig. 9. Desired shapes of T12-R obtained by simulation for PD- and DP-steps in different views. Notice that the ground projections of centers of mass (represented by blue stars) are located outside of the base rectangles.

Sect. II, and its controller design for dynamic locomotion is currently an ongoing research. In this section, a potential approach for the controller design is outlined.

In the biped locomotion research, the dynamic counterpart of GCoM is called *Zero Moment Point (ZMP)*, the concept of which is widely used to develop controllers for dynamic locomotion of bipeds [36], [37], [38], [39], [40]. By definition, ZMP is a point on the ground where the tipping moment due to the gravity and inertia forces is zero [41], [42], [43]. The tipping moment is the moment that is perpendicular to a sagittal plane and tangential to a supporting polygon. If ZMP is located inside of a supporting polygon, the tipping moment is balanced out by the ground reaction force. On the other hand, if ZMP is located outside of a supporting polygon, the tipping moment becomes nonzero and the system will tip over. Therefore, one of the main control objectives for biped locomotion is to keep ZMP within the biped's supporting polygon. In other words, because bipeds are naturally unbalanced systems, control efforts are made to keep them balanced by having ZMP within their supporting polygons.

T12-R, however, has the opposite control goal. Because T12-R (and many other spherical tensegrity robots) is naturally well-balanced, control efforts should be made to make it unbalanced in order to realize steps. In terms of ZMP, this corresponds to pushing ZMP outside of a supporting polygon using structural deformation, similar to what has been done in Sect. IV to realize static locomotion. Therefore, the control problem of realizing dynamic locomotion of T12-R can be seen as a dual of that of bipeds, and the previous research on the ZMP-based locomotion controller design for bipeds [44] may be adopted for the controller development of T12-R.

Moreover, it was shown earlier that the motion of T12-R may be described on a two-dimensional plane instead of a three-dimensional space as long as the robot maintains its symmetry about the sagittal plane during deformation. This simplified dynamics model of T12-R will further facilitate the controller design and implementation.

VI. Conclusion

This work discussed the design and locomotion control of a novel spherical tensegrity robot, T12-R. To the best of authors' knowledge, T12-R is the first robot designed and prototyped based on a rhombicuboctahedron-like twelve-rod tensegrity structure, and its detailed hardware design was provided. When compared to other spherical tensegrity robots that are based on a six-rod tensegrity structure, the geometry of T12-R is more suitable for high speed rolling as it enables the robot to move in a straight line, thus preventing the loss of momentum associated with the zig-zag motion of the six-rod tensegrity robots. Furthermore, dynamics of T12-R may be written in a simplified form by exploiting the symmetry of the robot, which could be used to facilitate the development of locomotion controller.

With the goal of realizing static locomotion of T12-R, a simulation study was done to find desirable deformations of the robot. The simulation is based on two methods: dynamic relaxation and multi-generation Monte Carlo. The simulation results showed that the current prototype of T12-R, although being underactuated, can deform its shape to perform desired steps. The hardware and control implementation of the actuation policies obtained from the simulation study is currently work in progress. Control strategies based on the concept of Zero Moment Point for achieving dynamic locomotion in hardware were presented and challenges that are unique to tensegrity robots were discussed.

References

[1] A. K. Agogino, V. SunSpiral, and D. Atkinson, "Super Ball Bot – structures for planetary landing and exploration," *NASA Innovative Advanced Concepts (NIAC) Program, Phase 1, Final Report*, Jul. 2013.

[2] K. Kim, L.-H. Chen, B. Cera, M. Daly, E. Zhu, J. Despois, A. K. Agogino, V. SunSpiral, and A. M. Agogino, "Hopping and rolling locomotion with spherical tensegrity robots," in *Proceedings of 2016 IEEE/RSJ International Conference on Intelligent Robots and Systems*. IEEE, 2016, pp. 4369–4376.

[3] R. B. Fuller, "Tensile-integrity structures," Patent US 3 063 521A, Nov. 13, 1962.

[4] C. Sultan, "Tensegrity: 60 years of art, science, and engineering," *Advances in applied mechanics*, vol. 43, pp. 69–145, 2009.

[5] C. Paul, F. J. Valero-Cuevas, and H. Lipson, "Design and control of tensegrity robots for locomotion," *IEEE Transactions on Robotics*, vol. 22, no. 5, pp. 944–957, 2006.

[6] Y. Koizumi, M. Shibata, and S. Hirai, "Rolling tensegrity driven by pneumatic soft actuators," in *Proceedings of 2012 IEEE International Conference on Robotics and Automation*. IEEE, 2012, pp. 1988–1993.

[7] V. Boehm, A. Jentzsch, T. Kaufhold, F. Schneider, F. Becker, and K. Zimmermann, "An approach to locomotion systems based on 3d tensegrity structures with a minimal number of struts," in *Proceedings of the 7th German Conference on Robotics (ROBOTIK 2012)*. VDE, 2012, pp. 1–6.

[8] K. Caluwaerts, J. Despraz, A. Işçen, A. P. Sabelhaus, J. Bruce, B. Schrauwen, and V. SunSpiral, "Design and control of compliant tensegrity robots through simulation and hardware validation," *Journal of The Royal Society Interface*, vol. 11, no. 98, 2014.

[9] K. Kim, A. K. Agogino, D. Moon, L. Taneja, A. Toghyan, B. Dehghani, V. SunSpiral, and A. M. Agogino, "Rapid prototyping design and control of tensegrity soft robot for locomotion," in *Proceedings of 2014 IEEE International Conference on Robotics and Biomimetics (ROBIO2014)*, Bali, Indonesia, Dec. 2014, *Best Student Paper Finalist*.

[10] L.-H. Chen, K. Kim, E. Tang, K. Li, R. House, E. Jung, A. K. Agogino, V. SunSpiral, and A. M. Agogino, "Soft spherical tensegrity robot design using rod-centered actuation and control," in *Proceedings of the ASME 2016 International Design Engineering Technical Conferences and Computers and Information in Engineering Conference 40th Mechanisms and Robotics Conference*. American Society of Mechanical Engineers, 2016.

[11] S. Lessard, D. Castro, W. Asper, S. Chopra, L. B. Baltaxe-Admony, V. SunSpiral, M. Teodorescu, and A. K. Agogino, "A bio-inspired tensegrity manipulator with multi-DOF, structurally compliant joints," in *Proceedings of 2016 IEEE/RSJ International Conference on Intelligent Robots and Systems*. IEEE, 2016.

[12] B. R. Tietz, R. W. Carnahan, R. J. Bachmann, R. D. Quinn, and V. SunSpiral, "Tetraspine: Robust terrain handling on a tensegrity robot using central pattern generators," in *Proceedings of 2013 IEEE/ASME International Conference on Advanced Intelligent Mechatronics*. IEEE, 2013, pp. 261–267.

[13] J. M. Friesen, P. Glick, M. Fanton, P. Manovi, A. Xydes, T. Bewley, and V. Sunspiral, "The second generation prototype of a duct climbing tensegrity robot, DuCTTv2," in *Proceedings of 2016 IEEE International Conference on Robotics and Automation*. IEEE, 2016, pp. 2123–2128.

[14] A. P. Sabelhaus, J. Bruce, K. Caluwaerts, P. Manovi, R. F. Firoozi, S. Dobi, A. M. Agogino, and V. SunSpiral, "System design and locomotion of SUPERball, an untethered tensegrity robot," in *Proceedings of 2015 IEEE International Conference on Robotics and Automation*. IEEE, 2015, pp. 2867–2873.

[15] J. Bruce, A. P. Sabelhaus, Y. Chen, D. Lu, K. Morse, S. Milam, K. Caluwaerts, A. M. Agogino, and V. SunSpiral, "SUPERball: Exploring tensegrities for planetary probes," in *Proceedings of 12th International Symposium on Artificial Intelligence, Robotics and Automation in Space (i-SAIRAS 2014)*, Montreal, Canada, Jun. 2014.

[16] J. Bruce, K. Caluwaerts, A. Iscen, A. P. Sabelhaus, and V. SunSpiral, "Design and evolution of a modular tensegrity robot platform," in *Proceedings of 2014 IEEE International Conference on Robotics and Automation*, 2014.

[17] A. P. Sabelhaus, J. Bruce, K. Caluwaerts, Y. Chen, D. Lu, Y. Liu, A. K. Agogino, V. SunSpiral, and A. M. Agogino, "Hardware design and testing of SUPERball, a modular tensegrity robot," in *Proceedings of The 6th World Conference of the International Association for Structural Control and Monitoring (6WCSCM)*, Barcelona, Spain, Jul. 2014.

[18] M. Shibata, F. Saijyo, and S. Hirai, "Crawling by body deformation of tensegrity structure robots," in *Proceedings of 2009 IEEE International Conference on Robotics and Automation*. IEEE, 2009, pp. 4375–4380.

[19] S. Hirai, Y. Koizumi, M. Shibata, M. Wang, and L. Bin, "Active shaping of a tensegrity robot via pre-pressure," in *Proceedings of 2013 IEEE/ASME International Conference on Advanced Intelligent Mechatronics*. IEEE, 2013, pp. 19–25.

[20] M. Khazanov, J. Jocque, and J. Rieffel, "Evolution of locomotion on a physical tensegrity robot," in *ALIFE 14: The Fourteenth Conference on the Synthesis and Simulation of Living Systems*, 2014, pp. 232–238.

[21] W. Du, S. Ma, B. Li, M. Wang, and S. Hirai, "Dynamic simulation for 6-strut tensegrity robots," in *Proceedings of 2014 IEEE International Conference on Information and Automation*. IEEE, 2014, pp. 870–875.

[22] A. Iscen, A. Agogino, V. SunSpiral, and K. Tumer, "Flop and roll: Learning robust goal-directed locomotion for a tensegrity robot," in *Proceedings of 2014 IEEE/RSJ International Conference on Intelligent Robots and Systems*. IEEE, 2014, pp. 2236–2243.

[23] M. Cefalo and J. M. Mirats-Tur, "A comprehensive dynamic model for class-1 tensegrity systems based on quaternions," *International Journal of Solids and Structures*, vol. 48, no. 5, pp. 785–802, 2011.

[24] R. E. Skelton, "Dynamics of tensegrity systems: Compact forms," in *Proceedings of the 45th IEEE Conference on Decision and Control*. IEEE, 2006, pp. 2276–2281.

[25] C. Sultan, M. Corless, and R. E. Skelton, "Linear dynamics of tensegrity structures," *Engineering Structures*, vol. 24, no. 6, pp. 671–685, 2002.

[26] N. Kanchanasaratool and D. Williamson, "Modelling and control of class nsp tensegrity structures," *International Journal of Control*, vol. 75, no. 2, pp. 123–139, 2002.

[27] A. S. Wroldsen, M. C. De Oliveira, and R. E. Skelton, "Modelling and control of non-minimal non-linear realisations of tensegrity systems," *International Journal of Control*, vol. 82, no. 3, pp. 389–407, 2009.

[28] K. Nagase and R. E. Skelton, "Network and vector forms of tensegrity system dynamics," *Mechanics Research Communications*, vol. 59, pp. 14–25, 2014.

[29] S. Faroughi, H. H. Khodaparast, and M. I. Friswell, "Non-linear dynamic analysis of tensegrity structures using a co-rotational method," *International Journal of Non-Linear Mechanics*, vol. 69, pp. 55–65, 2015.

[30] K. Kim, A. K. Agogino, A. Toghyan, D. Moon, L. Taneja, and A. M. Agogino, "Robust learning of tensegrity robot control for locomotion through form-finding," in *Proceedings of 2015 IEEE/RSJ International Conference on Intelligent Robots and Systems (IROS)*. IEEE, 2015, pp. 5824–5831.

[31] R. E. Skelton and M. C. de Oliveira, *Tensegrity systems*. Springer, 2009.

[32] M. Barnes, "Form-finding and analysis of prestressed nets and membranes," *Computers & Structures*, vol. 30, no. 3, pp. 685–695, 1988.

[33] M. R. Barnes, "Form finding and analysis of tension structures by dynamic relaxation," *International journal of space structures*, vol. 14, no. 2, pp. 89–104, 1999.

[34] L. Zhang, B. Maurin, and R. Motro, "Form-finding of nonregular tensegrity systems," *Journal of Structural Engineering*, vol. 132, no. 9, pp. 1435–1440, 2006.

[35] G. Fagerström, "Dynamic relaxation of tensegrity structures," in *Proceedings of the 14th International Conference on Computer Aided Architectural Design Research in Asia/Yunlin (Taiwan)*, vol. 22, 2009, pp. 553–562.

[36] S. Kajita, F. Kanehiro, K. Kaneko, K. Fujiwara, K. Harada, K. Yokoi, and H. Hirukawa, "Biped walking pattern generation by using preview control of zero-moment point," in *Proceedings of 2003 IEEE International Conference on Robotics and Automation*, vol. 2. IEEE, 2003, pp. 1620–1626.

[37] Y. Fujimoto and A. Kawamura, "Proposal of biped walking control based on robust hybrid position/force control," in *Proceedings of 1996 IEEE International Conference on Robotics and Automation*. IEEE, 1996, pp. 2724–2730.

[38] K. Hirai, M. Hirose, Y. Haikawa, and T. Takenaka, "The development of honda humanoid robot," in *Proceedings of 1998 IEEE International Conference on Robotics and Automation*, vol. 2. IEEE, 1998, pp. 1321–1326.

[39] P. Sardain and G. Bessonnet, "Zero moment point-measurements from a human walker wearing robot feet as shoes," *IEEE Transactions on Systems, Man, and Cybernetics-Part A: Systems and Humans*, vol. 34, no. 5, pp. 638–648, 2004.

[40] M. Vukobratović, B. Borovac, and D. Šurdilović, "Zero-moment point – proper interpretation and new applications," in *Proceedings of The Second IEEE-RAS International Conference on Humanoid Robots, CD-ROM*, 2001.

[41] P. Sardain and G. Bessonnet, "Forces acting on a biped robot. center of pressure – zero moment point," *IEEE Transactions on Systems, Man, and Cybernetics-Part A: Systems and Humans*, vol. 34, no. 5, pp. 630–637, 2004.

[42] M. Vukobratovic, A. Frank, and D. Juricic, "On the stability of biped locomotion," *IEEE Transactions on Biomedical Engineering*, no. 1, pp. 25–36, 1970.

[43] M. Vukobratović and B. Borovac, "Zero-moment point – thirty five years of its life," *International Journal of Humanoid Robotics*, vol. 1, no. 01, pp. 157–173, 2004.

[44] S. Kajita, H. Hirukawa, K. Harada, and K. Yokoi, *Introduction to humanoid robotics*. Springer, 2014, vol. 101.